Anal. Bioanal. Electrochem., Vol. 14, No. 3, 2022, 303-318

Analytical & Bioanalytical Electrochemistry

2022 by CEE
www.abechem.com

Full Paper

Electrochemical Examination of an Eco-friendly Corrosion Inhibitor "Almond Flower Extract" for Carbon Steel in Acidic Medium (1 M HCl)

Sara Lahmady,[1] Omar Anor,[1] Issam Forsal,[1,*] Hafida Hanin,[2] and Kalid Benbouya[3]

[1]*Laboratory of Engineering and Applied Technologies, School of Technology, Beni Mellal, Morocco*

[2]*Laboratory of Bioprocess and Biointerface, University Sultan Moulay Slimane, Faculty of Sciences and Technologies, Beni Mellal, Morocco*

[3]*EMDD_CERNE2D, Mohammed V University in Rabat, EST Salé, Morocco*

*Corresponding Author, Tel.: +212661118208

E-Mail: forsalissam@yahoo.fr

Received: 8 September 2021 / Received in revised form: 18 March 2022
Accepted: 20 March 2022 / Published online: 31 March 2022

Abstract- Green inhibitors have recently captured the attention of researchers to achieve good performance to inhibit and minimize corrosion with low environmental effects. For this reason, in this work, Almond flower extract (AFE) was used as a natural inhibitor to reduce the corrosion rate of carbon steel in an aggressive solution 1M HCl. The inhibition efficiency (IE%) of this extract was examined via different experimental methods such as Potentiodynamic polarization (PDP) and Electrochemical impedance spectroscopy (EIS) for five concentrations from 0.5 to 2.5 g/L. The outcomes denoted that the inhibitory impact increased with the rising concentration of flower extract up to 2.5 g/L and subsequently decreased with increasing concentration. PDP results reveal that (AFE) is a mixed-type corrosion inhibitor, the adsorption of this flower extract compounds followed the Langmuir isotherm, and its (IE%) of 2.5g/L (AFE) can exceed 96% at 293 K. The inhibitory impact of Almond flower extract was studied at different temperatures ranging from 293 K to 323 K. The inhibition performance of (AFE) remained virtually constant with rising immersion time, depending on the results of the EIS.

Keywords- Almond flower extract (AFE); Immersion time; corrosion; carbon steel; Langmuir

1. INTRODUCTION

Metal equipment used in industrial activities is generally exposed to the phenomenon of corrosion [1,2]. Surface treatment by acid pickling, cleaning of heat exchangers, acid-descaling, are some of the processes which use very acidic solutions, in particular hydrochloric acid [3–5]. This aggressive media certainly leads to a failure which causes economic losses and can affect the quality of the product [2]. For this reason, there is always a search for an effective solution to decrease the corrosion rate of metallic components, especially steel metal in an acidic environment [1].

Among the available methods to prevent and control corrosion, the use of synthetic corrosion inhibitors such as inorganics inhibitors (nitrates, phosphates, chromates) [6–8], and organic inhibitors (triazole, imidazole compounds, polyamines) [9–13].

These compounds are effective but also expensive and toxic to the environment which creates an ecological imbalance and they are dangerous for human health [14]. Therefore, it is necessary to search for corrosion inhibitors with an excellent environmental profile [15]. Natural substances are suitable candidates to replace synthetic inhibitors. They are biodegradable, Eco-friendly, easily available, and inexpensive [16].

Extracts from parts of plants such as bark, leaves, fruits, skin, seeds, roots, and flowers are widely used as green corrosion inhibitors [17]. Several studies have shown that this kind of inhibitor generally has high inhibition efficiency and a good performance due to the existence of complex organic species such as amino acids, carbohydrates, proteins, polyphenolic compounds, etc [18]. Heteroatoms like nitrogen, sulfur, oxygen, and phosphorus, as well as aromatic functional groups enriched with π electrons, are commonly found in these compounds [19,20]. This permits them to adsorb on the substrate's surface and produce a protective coating that functions as a barrier against acid damage [21]. The protective effect is frequently linked to chemical and/or physical adsorption, which implies a modification in the charge of the adsorbed material [22].

Natural plants as corrosion inhibitors of steel metal have been subjected to many investigations, for example: Dates Extracts [23], Oil of J. Juniperus Phoenicea [24], Bamboo leaf extract [25], Ginko leaves extract [26], Citrullus Lanatus Fruit Extract [27], Borage Flower Aqueous Extract [28], Pineapple Stem Extract [29], Lagerstroemia Speciosa Leaf Extract [30], Essential Oil of Lavandula [31], and leaf extract of Elaeis Guineensis [32].

The outcomes reveal that these plants are great natural inhibitors for preventing corrosion of steel in an acidic medium. As stated in the literature the effectiveness of corrosion inhibition generally controlled by the amount of inhibitor, the temperature of the solution, the immersion time and the nature of the aggressive medium [20].

In the same direction, to respond to the interest in environmental and ecological corrosion inhibitors, the effect of Almond flower extract on the corrosion of carbon steel in acidic solution (HCl 1M) was investigated in this study. Electrochemical impedance spectroscopy (EIS) and

potentiodynamic polarization were used to examine the inhibition effect of (AFE) on the corrosion of the metal used. In this work, we have controlled different parameters which have an important impact on the corrosion phenomenon such as the concentration of AFE, the immersion time, and the temperature.

2. MATERIALS AND METHODS

2.1. Preparation of Electrode and Solution

Working electrode used in the following study is composed of C (0.07%), Mn (0.19%), Si (0.03%), Cr (0.05%), Al (0.02%) and the remaining is Fe. It was supplied by the Moroccan Iron and Steel Company. The specimens were cut into a rectangular shape of dimension 0.8 cm × 4 cm × 0.2 cm. Prior each experiment, the surface of the working electrode was polished with different grades (180,200,400,600, 1200, 1500, and 2000) of grit silicon carbide (SiC) emery papers, then it is degreased with acetone and washed abundantly with distilled water, and dried before conducting an experiment. Hydrochloric acid grad 37 % from MERCK was diluted with distilled water to prepare the corrosive solution 1M HCl. A volume of 25 mL of dilute hydrochloric acid was used to ensure good immersion of the electrodes in the electrochemical cell. After each sweep, a new solution and carbon steel samples were used.

2.2. Preparation of Corrosion Inhibitor

The almond flowers were collected from Chichaoua region, Marrakech, at the end of February. The fresh flowers were washed to eliminate dust, and dried for 15 days in shade at room temperature (25°C- 27 °C). The dried flowers material was crushed into powder using a blender. The extraction was carried out using the technique of maceration in ethanol. The powdered sample (5 g) was added to 100 mL of ethanol with stirring for 48 hours at room temperature and protected from light. A rotary evaporator was used to concentrate the filtered product at a temperature 45 ° C. Inhibitor solutions with different concentrations of Almond flower extract such as, 0.5, 1, 1.5, 2, 2.5, 3 g/L were prepared in 1 M HCl.

2.3. Electrochemical Measurements

All electrochemical Experiments of this study were accomplished using potentiostat OrigaStat 100, equipped with origamaster5 software. The typical three-electrode cell was used, consisting of a working electrode made of carbon steel with an exposed area of 0.64 cm^2, a platinum as the counter electrode and a saturated calomel electrode (SCE) as the reference electrode. The coupon was immersed in the corrosive solutions for 30 minutes before measurements to obtain a stable state open circuit potential (E_{ocp}). Potentiodynamic polarization curves were acquired in the potential range of -750 to -100 mV relative to the (SCE) reference electrode with the scan rate of 1 $mV.s^{-1}$, starting from cathodic to anodic

direction. To support PDP data the Electrochemical Impedance was carried out at open circuit potential (Eocp) at the frequency range from 100 mHz to 1kHz by applying the signals of sine wave voltage of 0.01 V peak to peak. The impedance diagrams are given as Nyquist representations. The results were fitted by using EC-Lab software. The impact of temperature on the inhibitor performance was controlled in a temperature range of 293 -323 K.

3. RESULTS AND DISCUSSION

3.1. Potentiodynamic Polarization Measurements (PDP)

Cathodic and anodic polarization curves for carbon steel specimens in 1 M HCl solution with and without Almond flower extract at five different concentrations at 293 K are given in Figure 1. The Tafel extrapolation way was applied to obtain the electrochemical parameters including the values of corrosion current density (I_{corr}), corrosion potential (Ecorr), cathodic Tafel slope (b_c), anodic Tafel slope (b_a), surface coverage (θ), and inhibition efficiency (IE%). The outcomes are grouped in Table 1. Using the equation (1) below, the inhibition efficiency values were determined from the Icorr data [33–35]:

$$(\text{IE}\%) = \frac{\text{Icorr} - \text{I}'\text{corr}}{\text{Icorr}} * 100 \qquad (1)$$

where I_{corr} is the corrosion current density without the inhibitor and I'_{corr} is the corrosion current density with the inhibitor.

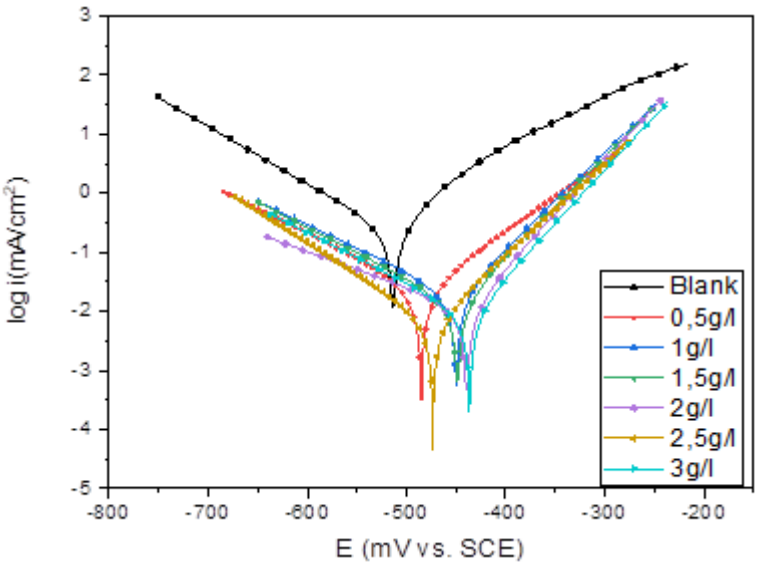

Figure 1. Polarization curves for carbon steel in 1 M HCl in the absence and presence of various concentrations of AFE at 293 K

As shown in Figure 1, the addition of the AFE to the corrosive medium is accompanied by a displacement of E_{corr} towards a positive potential direction. Furthermore, as can be seen both

the anodic and the cathodic reactions are inhibited. So, the almond flower extract works as a mixed type inhibitory action with a predominant anodic impact.

According to the data provided in Table 1, corrosion current density decreases in the presence of the inhibitor, starting from 174.7 up to a value of 6.421 µA/cm^2 at 2.5g/L at 293 K. This activity is caused by inhibitory molecules that bind to active sites on the surface of the steel [36,37]. With increasing inhibitor concentration, the inhibition efficiency (IE %) increases until it reaches 96% at 2.5 g/L of AFE.

Table 1. Electrochemical parameters determined from polarization measurements for carbon steel in 1 M HCl solution in the absence and presence of various concentrations of AFE at 293 K

Concentration (g/L)	I_{corr} (µA/cm^2)	$-E_{corr}$ (mV vs SCE)	b_a (mV/dec)	$-b_c$ (mV/dec)	IE (%)	θ
Blank	174.4	513.7	58.6	88.6		
0,5	24.179	485.078	86.5	121.3	86.13	0.86
1	18.988	449.926	62.2	126.5	89.11	0.89
1,5	13.366	448.552	59.4	116.9	92.33	0.92
2	11.216	439.348	55.6	166.9	93.56	0.93
2,5	6.421	473.511	64.7	93.9	96.31	0.96
3	8.658	437.1	55.4	117.3	95.01	0.95

If the potential corrosion displacement against the blank is larger than 85 mV, the inhibitor is known to be anodic or cathodic, however if the offset is less than 85 mV, the inhibitor is known to be mixed [38–40]. In the following study the maximum corrosion potential of steel was changed to 36 mV anodically in comparison to the blank, which suggested that the inhibitor is a mixed type. In other words, anodic steel dissolution both and cathodic hydrogen evolution were retarded by the existence of inhibitor in the corrosive environment [41]. A similar shift in Ecorr values has been reported in the literature, and the inhibitor is regarded to be a mixed type inhibitor with anodic predominance [42–44].

3.2. Electrochemical Impedance Spectroscopy (EIS)

Figure 2 reveals Nyquist plots of carbon steel in 1M HCl solution in the absence and in the existence of various concentrations of Almond flower extract during the exposition time of 30 min at 293k. Examination of Nyquist diagrams shows that the impedance response of the carbon steel in uninhibited acid solution changed considerably after the addition of AFE into the aggressive solution. The presence of a single capacitive loop implies that the corrosion mechanism is primarily regulated by a charge transfer process [45,46]. The forms of the

semicircles in the uninhibited and inhibited solutions were identical, indicating that the mechanism of steel corrosion is unaffected by the addition of inhibitors [46].

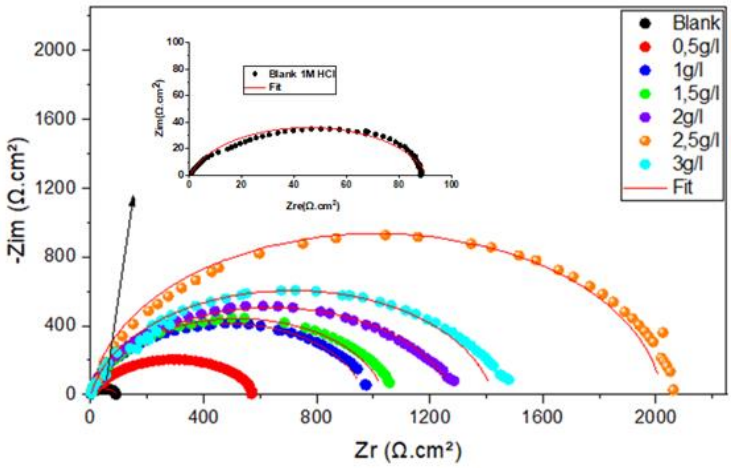

Figure 2. Nyquist plots for carbon steel in 1 M HCl in the absence and presence of various concentrations of AFE at 293 K

The size of the capacitive loop was increased when the amount of almond flower extract was enhanced, according to the impedance diagrams. The semicircles in the Nyquist plots are obviously imperfect; this behavior is commonly attributed to metal surface inhomogeneity caused by surface roughness or interfacial phenomena [47,48].

The high agreement between the fitting lines and experimental plots indicates the correctness of the EIS measurements (Figure 2). The excellent quality of the fit denotes a good correlation with the equivalent circuit model (Figure 3). A similar equivalent circuit was used by other research to describe iron/acid interface [6,49,50].

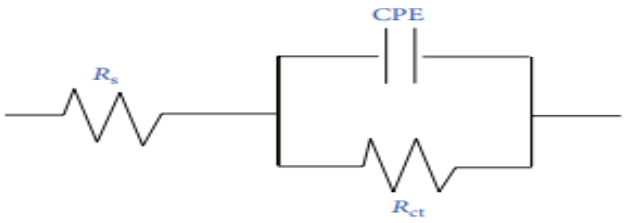

Figure 3. Equivalent electrical circuit of the interface of carbon steel/HCl electrolyte

The model in Figure 3 consists of electrolyte resistance R_s, charge transfer resistance R_{ct}, and constant phase element CPE which is placed in parallel to R_{ct} element. Indeed, in these cases, to give a more accurate, pure double layer capacitors C_{dl} are best described by a transfer function with constant phase elements (CPE) and the following equation gives its impedance [51,52]:

$$Z_{CPE} = \frac{1}{\mathrm{A}}(j\omega)^{-n} \qquad (2)$$

where Z_{CPE} = CPE impedance, A= CPE constant, ω= angular frequency, j= imaginary number (i.e. $i^2 = -1$), and n= phase shift exponent that is a measure of surface irregularity/ inhomogeneity [20]. For plane and homogeneous electrode with a regular surface, when n=1, CPE can be considered as a real capacitor [53]. The difference in impedance at lower and higher frequencies is used to calculate the charge transfer resistance (R_{ct}) values. The inhibitory efficiency was obtained for EIS investigation using equation (3) [54]:

$$(IE\%) = \frac{R_{ct} - R_{ct0}}{R_{ct}} * 100 \qquad (3)$$

where R_{ct} and R_{ct0} are charge transfer resistance in existence and absence of inhibitor obtained from the electrochemical impedance diagrams.

It is clear from Table 2 that (R_{ct}) enhanced with the raising of the flower extract concentrations, this is attributed to the construction of a protective film on the metal solution interface owing to the adsorption of the inhibitor on the most active adsorption sites [55]. As the concentration of almond leaf extract increases, the value of (IE%) rises, indicating that the film formed by AFE in the carbon steel surface becomes denser and more ordered. When the flower extract is 2.5g/L, the corrosion inhibition efficiency can reach over 95%. In addition, the value of C_{dl} shows a downward trend with increasing AFE concentration, the addition of this inhibitor decreases the C_{dl} double layer capacitance values from 211.3 to 21.7 µF/cm^2. The reduction in Cdl is attributed to the decrease in the dielectric constant and the rise in the density of the electrical double layer [56]. According to the literature, the reduction in C_{dl} values is caused by the displacement of water molecules at the metal solution interface by the adsorbed inhibitor molecule, enabling a protective layer to develop on the steel surface [57,58].

Table 2. The electrochemical impedance spectroscopy parameters for carbon steel in 1 M HCl solution in the absence and presence of various concentrations of AFE AT 293K

Concentration (g/L)	R_s (Ω.cm^2)	R_{ct} (Ω.cm^2)	C_{dl} (µF.cm^{-2})	n	Q_{dl} (µΩ^{-1} cm^{-2} S^n)	IE(%)
Blank	0.623	87.78	211.3	0.88	340	
0.5	0.025	589.8	74.82	0.76	154.4	85.11
1	0.156	953.2	46.16	0.76	95.47	90.68
1.5	0.418	1 037	42.66	0.76	88.22	91.53
2	0.266	1 285	40.8	0.84	63.51	93.16
2.5	0.163	2 027	21.76	0.76	45.05	95.65
3	0.385	1 422	33.22	0.89	45.3	93.82

3.3. Adsorption Isotherm

The adsorption isotherm may be used to characterize the adsorption process of corrosion inhibition. This study provides information about the interaction of AFE inhibitor with active sites on metal surface [59]. Therefore, in order to predict which mechanism AFE was adsorbed on the metal surface at 293 K, various adsorption isotherm models were investigated, including, Temkin, Langmuir, El-Awady, Flory-Huggins, Freundlich, Frumkin, and Temkin (Figure 4). Their expressions are summarized in Table 3 [16,60]. The best suitable model to fit our experimental data was Langmuir isotherm. The Langmuir model is generally based on model assumptions that all active sites have equal energy distributions, that only monolayer adsorption occurs, and that molecules at adjacent sites do not interact [46].

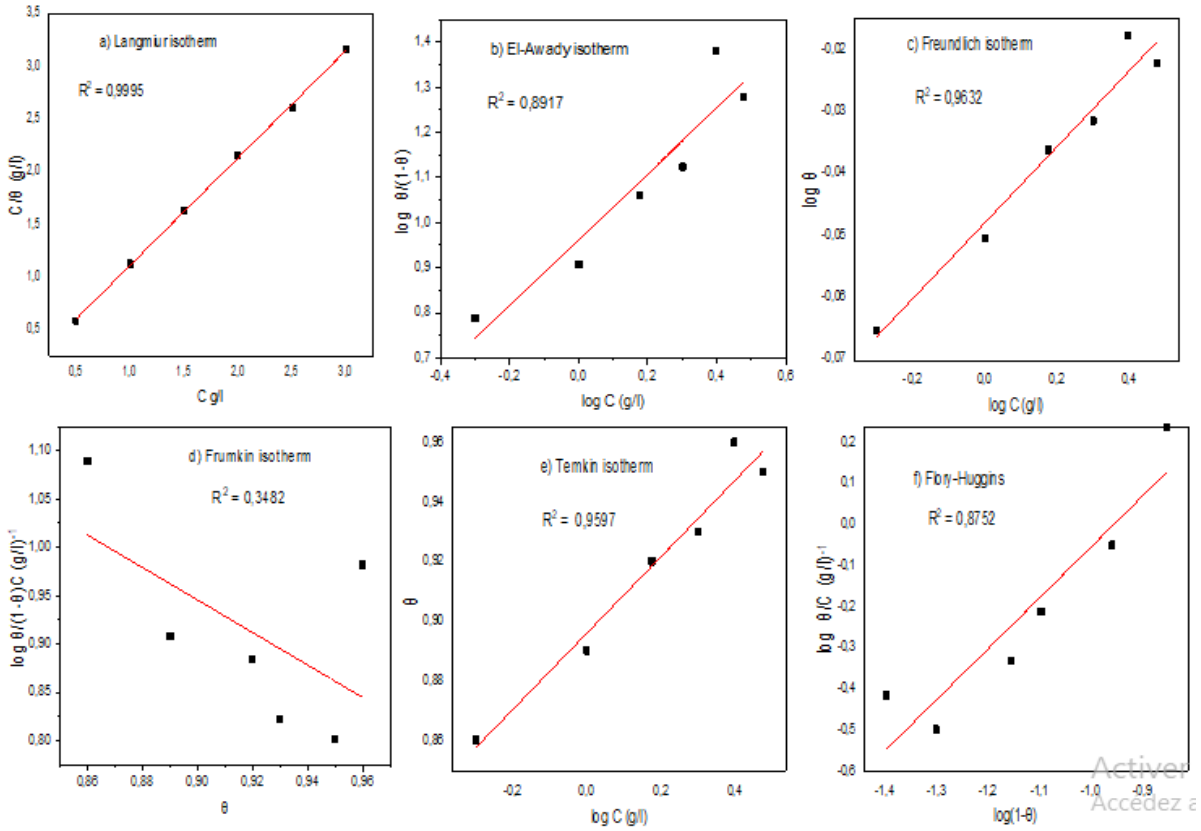

Figure 4. Fitting results of various isothermal adsorption curves for PDP curve data: (a) Langmuir, (b) El-Awady, (c) Freundlich, (d) Frumkin, (e) Temkin, and (f) Flory-Huggins

Where θ is the surface coverage, C_{inh} is the inhibitor concentration, and K_{ads} the standard adsorption equilibrium constant. Figure 4 exhibits the linear relationships for all tested adsorption models of AFE at 293k. The good fit between experimental points and calculated lines with regression coefficient (R^2=0.999) asserts that the adsorption of this extract on metal surface obeys Langmuir adsorption model.

Table 3. Models of isotherms and their linear forms

Isotherm	Linear form	Plot
Langmiur	$\frac{C}{\theta} = \frac{1}{K_{ads}} + C$	$\frac{C}{\theta}\ vs. C$
El-Awady	$log\ \frac{\theta}{1-\theta} = \mathrm{y}\log C + logK$	$Log\ \frac{\theta}{1-\theta}\ vs. \log C$
Freundlich	$log\ \theta = \mathrm{n}\log C + logK_{ads}$	$log\ \theta\ vs. \log C$
Frumkin	$ln\ \frac{\theta}{(1-\theta)C} = \mathrm{lnK} + 2\alpha\theta$	$ln\ \frac{\theta}{(1-\theta)C}\ vs. \theta$
Temkin	$\theta = \left(\frac{2.303}{\alpha}\right)(logK_{ads} + \log C)$	$\theta\ vs. \log C$
Flory-Huggins	$log\ \frac{\theta}{C} = \mathrm{x}\log(1-\theta) + \log(xK_{ads}$	$log\ \frac{\theta}{C}\ vs. \log(1-\theta)$

3.4. Effect of Temperature on Corrosion Inhibition

The corrosion phenomenon is inevitably affected by temperature, this parameter impacts the mechanism of inhibitor adsorption i.e. the active compounds may undergo decomposition and/ or rearrangement [46,61]. The polarization measurements were used at different temperatures from 293 K to 323 K to examine the effect of this factor on the corrosion rate of steel in the 1M HCl medium with 2.5 g/L of Almond flower extract as the optimal concentration that corresponds to the best inhibition efficiency (Figure 5). The electrochemical parameters of polarization curves are summarized in Table 4.

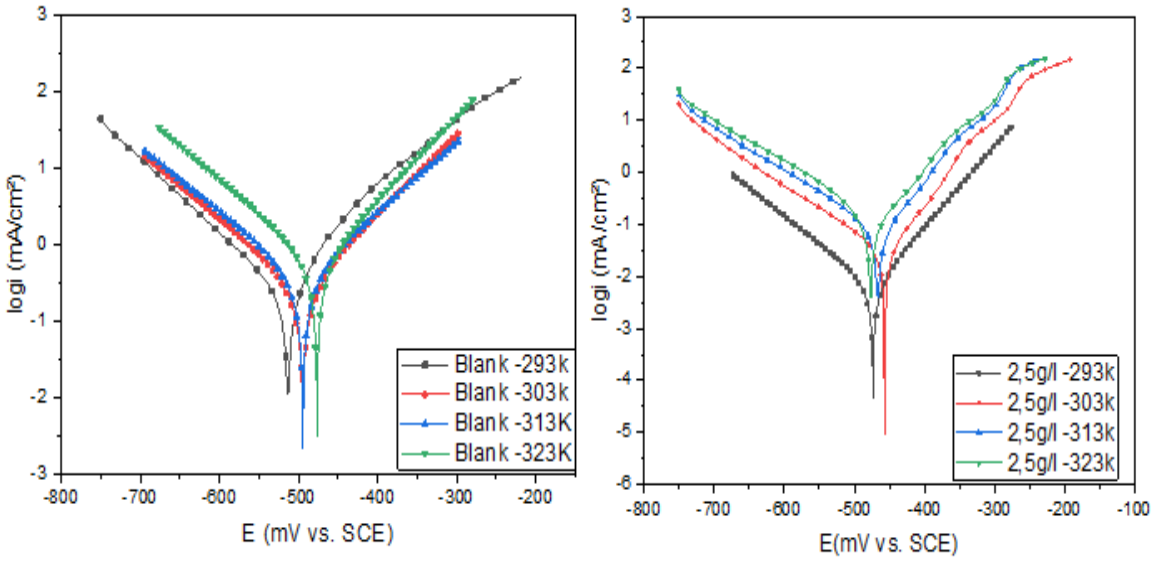

Figure 5. Polarization curve for carbon steel immersed in 1 M HCl and 1 M HCl + 2.5 g/l of AFE at different ranges of temperature

Table 4. Electrochemical parameters determined from polarization measurements for carbon steel immersed in 1 M HCl and 1 M HCl + 2.5 g/L of AFE at different ranges of temperature

	T (K)	I_{corr} (µA/cm^2)	-E_{corr} (mV vs SCE)	b_a (mV/dec)	-b_c (mV/dec)	IE (%)
Blank	293	174.4	513.7	58.6	88.6	
	303	269.043	494.723	96.8	115.5	
	313	373.612	494.546	110.2	121.4	
	323	595.896	476.517	93.1	114.1	
2.5 g/L of AFE	293	6.421	473.511	64.7	93.9	96.32
	303	34.6	456.8	69.5	119.2	87.14
	313	80.2	466.5	64.7	119.7	78.53
	323	196.5	476.9	81.6	131.9	67.02

The outcomes indicate that I_{corr} for carbon steel used increased with elevation of temperature for blank media and in the existence of 2.5 g/L of inhibitor. Therefore, the IE% decreases strongly, it changed from 95% to 67%. This behavior indicates that the AFE molecules have been adsorbed to the steel surface by physisorption [62]. The temperature change was identified to be an effective factor influencing the corrosion kinetics of steel; it impacts the intensity of inhibitor adsorption on metal surfaces [26,63].

3.5. Effect of Immersion Time on Corrosion Inhibition

The immersion time is a significant factor to examine the steadiness of the inhibitory behavior; therefore, it is necessary to study this factor in order to assess the behavior of the element used as an inhibitor.

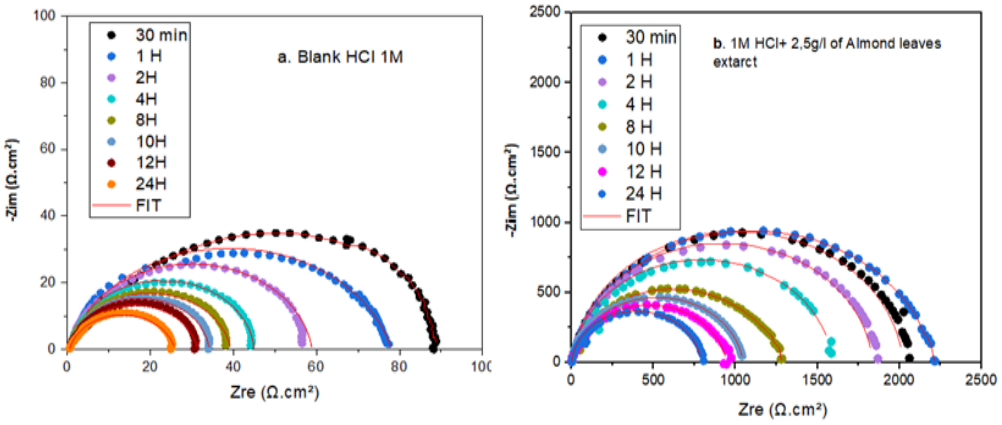

Figure 6. Nyquist plots for carbon steel immersed in a. 1 M HCl and b. 1 M HCl + 2.5 g/l of AFE at different times of immersion at 293 K

In order to investigate the evolution of the inhibitive performance of the extract used in this paper on an interval of time, EIS measurements were executed in 1 M HCl in the absence and existence of the 2.5 g/L AFE for (30 min, 1H, 2 H, 4H, 8 H, 10 H, 12 H, 24 H) immersion time at temperature 293 K.

Electrochemical impedance spectroscopy is used as a technique for long duration time tests because it does not significantly disturb the system and it is possible to follow its evolution over time [64]. EIS curves of steel substrate immersed in 1M HCl solution without and with 2.5g/L of AFE at different times from 30 min to 24 H were given in Figure 6. The inhibition efficiency and calculated parameters are grouped in Table 5.

Table 5. Electrochemical parameters for carbon steel immersed in 1 M HCl and 1 M HCl + 2.5 g/l of AFE at different times of immersion at 293K

	Immersion time	R_s ($\Omega.cm^2$)	R_{ct} ($\Omega.cm^2$)	C_{dl} ($\mu F.cm^{-2}$)	n	Q_{dl} ($\mu\Omega^{-1}$ cm^{-2} S^n)	IE (%)
Blank	30 min	0.623	87.78	211	0.88	340	
	1 H	0.205	77.86	118.6	0.84	247.6	
	2 H	0.959	57.99	261	0.92	363.4	
	4 H	1.06	43.91	365.2	0.96	425.9	
	8 H	0.694	38.64	472.5	0.91	669.6	
	10 H	0.701	33.46	569.1	0.94	697.1	
	12 H	0.552	31.6	760.8	0.89	1110	
	24 H	0.543	25.36	1510	0.87	2301	
2.5 g/L of AFE	30 min	0.163	2 027	21.76	0.76	45.05	95.67
	1 H	1.659	2148	37.26	0.95	41.84	96.38
	2 H	1.416	1 830	43.41	0.95	48.75	96.83
	4 H	0.2285	1592	50.51	0.94	57.31	97.24
	8 H	0.472	1240	51.67	0.91	65.95	96.88
	10 H	1.617	1045	52.23	0.92	64.88	96.80
	12 H	0.134	945.3	58.17	0.91	75.02	96.65
	24 H	0.485	633.6	127	0.95	143	96.00

As illustrated in Figure 6, the capacitive loops kept the same shape in blank medium, and in 2.5 g/L of AFE solution, the size of the impedance spectra was also influenced with increasing time. Table 5 exhibits that the R_{ct} decreased considerably with raising immersion time in the blank solution. When a concentration of 2.5 g/L of AFE is present, the inhibition efficiency remains nearly stable as exposure time increases. This behavior is mostly related to

the number of vacant sites, which are unoccupied when the steel is initially exposed to the inhibited environment. Therefore, the attractive forces between the active sites of the metal surface and the free electrons of the heteroatom molecules will appear which helps to improve the efficiency during the immersion time until full filling [65]. Therefore, we conclude that the inhibitor used in this work functions as a good barrier protecting the carbon steel over time.

3.7. Mechanism of Inhibition

Almond flower extract has been identified as a promising source of bioactive phytochemical [66]. As reported in previous studies, it contains phenolics, tannins, and flavonoids, as well as organically active components, including proanthocyanidins and volatile chemicals like eugenol, α-pinene and limonene [66, 70]. It revealed that trans-linalool oxide and carvacrol are the main volatile compounds in AFE [70]. Figure 7 shows the molecular structures of major volatile compounds in the Almond flower extract.

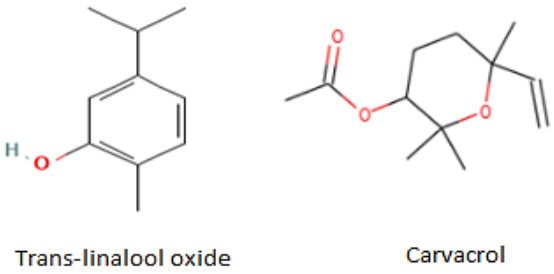

Figure 7. Major volatile compounds in the AFE

According to PDP and EIS measurements, Almond flower extract molecules were adsorbed on the carbon steel surface and developed a protective film layer that prevents the attack of water and HCl (H^+, Cl^-) ions, reducing the corrosion process significantly. As we mentioned before AFE is rich in organic compounds with heteroatom and π site in their molecular structures. Chemical substances of flower extract were adsorbed on the metal surface through interactions between free electrons of O-heteroatoms and vacant d-orbitals of iron atoms, and π -electrons of aromatic rings can also donate to the active site of iron atoms [1]. According to the temperature effect on the inhibition efficiency of AFE, the adsorption of this extract on the metal surface is physisorption. When inhibitor molecules are introduced into an acidic solution, they get protonated, and these protonated molecules are physically adsorbed on the surface through electrostatic interaction with Cl^- [1]. The adsorption via the synergistic effect of the majority elements as well as the minor components of the composition of the AFE inhibitor can be attributed to the inhibitory action of this flower extract [71].

4. CONCLUSION

Almond flower extract revealed a good performance as a natural corrosion inhibitor for carbon steel in aggressive solution 1 M HCl. From the polarization studies (PDP), it was clear that the inhibitory impact enhanced with the augmentation of inhibitor concentration, and this method showed that AFE used was a mixed type inhibitor. The highest efficiency value of 96% is obtained for a concentration of 2.5g/L AFE. The EIS graphs exhibited a single capacitive loop, suggesting that the charge transfer process controls the corrosion reaction. AFE acts as an effective barrier to protect the carbon steel surface during immersion time. However, when the temperature rises, the inhibitory efficiency decreases. The results obtained indicate a reasonable agreement between the Potentiodynamic polarization measurements and Impedance electrochemical measurements.

REFERENCES

[1] A. Pal, and C. Das, Industrial Crops and Products 151 (2020) 112468.
[2] K. Xhanari, M. Finšgar, M. Knez Hrnčič, U. Maver, Ž. Knez, and B. Seiti, RSC Adv. 7 (2017) 27299.
[3] Y. Elkhotfi, H. Boubekraoui, J. Zoubir, I. Forsal, and E. Rakib, Journal of Chemical Technology and Metal (2021) 6.
[4] C. Verma, E. E. Ebenso, I. Bahadur, and M. A. Quraishi, J. Mol. Liq. 266 (2018) 577.
[5] A. Singh, V. K. Singh, and M. A. Quraishi, Int. J. Corr. 2010 (2010) 1.
[6] M. W. Kendig, and R. G. Buchheit, Corr. 59 (2003) 379.
[7] L. Yohai, M. Vázquez, and M. B. Valcarce, Electrochim. Acta 102 (2013) 88.
[8] N. C. Rosero-Navarro, M. Curioni, R. Bingham, A. Durán, M. Aparicio, R. A. Cottis, and G. E. Thompson, Corr. Sci. 52 (2010) 3356.
[9] M. Goyal, S. Kumar, I. Bahadur, C. Verma, and E. E. Ebenso, J. Mol. Liq. 256 (2018) 565.
[10] M. Zunita, D. Wahyuningrum, Buchari, B. Bundjali, I. G. Wenten, and R. Boopathy, Applied Sci. 10 (2020) 7069.
[11] Y. Elkhotfi, I. Forsal, E. M. Rakib, and B. Mernari, Der Pharma Chemica 8 (2016) 160.
[12] Y. Elkhotf, I. Forsal, and E. Rakib, Der Pharma Chemica 9 (2017) 75.
[13] Y. Elkhotfi, M. E. Ghozlani, Y. Hakamaoui, I. Forsal, E. M. Rakib, and B. Mernari, American J. Eng. Res. 6 (2017) 247.
[14] S. A. Umoren, J. Adhesion Sci. Technol. 30 (2016) 1858.
[15] M. S. Yahya, G. Kaichouh, M. Khachani, M. E. Karbane, M. A. Arshad, A. Zarrouk, K. E. Kacemi, Anal. Bioanal. Electrochem, 12 (2020) 425.
[16] M. A. El-Hashemy, A. Sallam, J. Mater. Res. Technol. 9 (2020) 13509.
[17] R. Idouhli, A. Oukhrib, M. Khadiri, O. Zakir, A. Aityoub, A. Abouelfida, A. Benharref, and A. Benyaich, J. Mol. Structure 1228 (2021) 129478.

[18] A. A. S. Begum, R. M. A. Vahith, V. Kotra, M. R. Shaik, A. Abdelgawad, E. M. Awwad, and M. Khan, Coatings 11 (2021) 106.
[19] H. Wei, B. Heidarshenas, L. Zhou, G. Hussain, Q. Li, and K. Ostrikov, Materials Today Sustainability 10 (2020) 100044.
[20] L. T. Popoola, Corr. Rev. 37 (2019) 71.
[21] A. A. Ganash, Chem. Eng. Commun. 205 (2018) 350.
[22] M. Zunita, D. Wahyuningrum, B. B. Bundjali, I. G. Wenten, and R. Boopathy, Applied Sci. 10 (2020) 7069.
[23] H. Boubekraoui, I. Forsal, H. Ouradi, Y. Elkhotfi, and H. Hanin, Anal. Bioanal. Electrochem, 12 (2020) 828.
[24] Y. Elkhotfi, I. Forsal, E. M. Rakib, and B. Mernari, Port. Electrochim. Acta 36 (2018) 77.
[25] X. Li, S. Deng, and H. Fu, Corr. Sci. 62 (2012) 163.
[26] S. Deng, and X. Li, Corr. Sci. 55 (2012) 407.
[27] A. Dehghani, G. Bahlakeh, B. Ramezanzadeh, and M. Ramezanzadeh, J. Mol. Liq. 279 (2019) 603.
[28] A. Dehghani, G. Bahlakeh, B. Ramezanzadeh, and M. Ramezanzadeh, J. Mol. Liq. 277 (2019) 895.
[29] M. Mobin, M. Basik, and J. Aslam, Measurement 134 (2019) 595.
[30] M. Mobin, M. Basik, and Y. El Aoufir, J. Mol. Liq. 286 (2019) 110890.
[31] H. Boubekraoui, I. Forsal, M. Ellaite, K. Benbouya, and H. Hanin, Anal. Bioanal. Electrochem. 13 (2021) 80.
[32] M. A. Asaad, M. Ismail, N. H. A. Khalid, G. F. Huseien, and P. Bothi Raja, J. Teknol. 80 (2018).
[33] K. Muthukumarasamy, S. Pitchai, K. Devarayan, and L. Nallathambi, Materials Today: Proceedings 33 (2020) 4054.
[34] M. Manssouri, M. Znini, Y. E. Ouadi, A. Ansari, J. Costa, and L. Majidi, Anal. Bioanal. Electrochem. 12 (2020) 841.
[35] H. Lgaz, I. M. Chung, R. Salghi, I. H. Ali, A. Chaouiki, Y. El Aoufir, and M. I. Khan, Applied Surf. Sci. 463 (2019) 647.
[36] R. Solmaz, Corr. Sci. 81 (2014) 75.
[37] A. Sedik, D. Lerari, A. Salci, S. Athmani, K. Bachari, İ. H. Gecibesler, and R. Solmaz, J. Taiwan Inst. Chem. Eng. 107 (2020) 189.
[38] R. K. Pathak, and P. Mishra Int. J. Sci. Res. 5 (2016) 671.
[39] G. Ghenimi, M. Ouakki, H. Barebita, A.E. Fazazi, and M. Cherkaoui, Anal. Bioanal. Electrochem, 12 (2020) 20.
[40] R. Idouhli, A. Abouelfida, A. Benyaich, and A. Aityoub, Chem. Process Eng. Res. 44 (2016).

[41] M. A. Bidi, M. Azadi, M. Rassouli, Materials Today Commun. 24 (2020) 100996.
[42] P. Arockiasamy, X. Q. R. Sheela, G. Thenmozhi, M. Franco, J. W. Sahayaraj, and R. J. Santhi, Int. J. Corr. 2014 (2014) 1.
[43] L.O. Olasunkanmi, M. M. Kabanda, and E. E. Ebenso, Physica E 76 (2016) 109.
[44] D. Özkir, E. Bayol, A. A. Gürten, and Y. Sürme, J. Chil. Chem. Soc. 58 (2013) 2158.
[45] A. K. Singh, S. Mohapatra, and B. Pani, J. Industrial Eng. Chem. 33 (2016) 288.
[46] R. Idouhli, A. Oukhrib, Y. Koumya, A. Abouelfida, A. Benyaich, and A. Benharref, Corr. Rev. 36 (2018) 373.
[47] N. Karki, S. Neupane, Y. Chaudhary, D.K. Gupta, and A. P. Yadav, Anal. Bioanal. Electrochem. 12 (2020) 970.
[48] R. Solmaz, Corr. Sci. 52 (2010) 3321.
[49] A. S. Fouda, Int. J. Electrochem. Sci. (2017) 11397.
[50] C. Kamal, M. G. Sethuraman, Mater. Corr. 65 (2014) 846.
[51] E. Ituen, O. Akaranta, A. James, J. Taibah Univ. Sci. 11 (2017) 788.
[52] A. K. Satapathy, G. Gunasekaran, S. C. Sahoo, K. Amit, P. V. Rodrigues, Corr. Sci. 51 (2009) 2848.
[53] Y. Lin, A. Singh, E. E. Ebenso, Y. Wu, C. Zhu, H. Zhu, J. Taiwan Inst. Chem. Eng. 46 (2015) 214.
[54] A. M. Shah, Int. J. Electrochem. Sci. (2017) 9017.
[55] K. K. Anupama, K. Ramya, K. M. Shainy, and A. Joseph, Mater. Chem. Phys. 167 (2015) 28.
[56] T. Ibrahim, and M. Habbab, Int. J. Electrochem. Sci. 6 (2011) 16.
[57] N. K. Sebbar, Moroccan J. Heterocyclic Chem. 16 (2017) 1.
[58] H. Elmsellem, A. Elyoussfi, N. K. Sebbar, A. Dafali, K. Cherrak, H. Steli, E. M. Essassi, A. Aouniti, and B. Hammouti, Maghrebian J. Pure and Applied Sci. 1 (2015) 1.
[59] R. Idouhli, A. Oukhrib, M. Khadiri, O. Zakir, A. Aityoub, A. Abouelfida, A. Benharref, and A. Benyaich, J. Mole. Structure 1228 (2021) 129478.
[60] S. Chen, S. Chen, B. Zhu, C. Huang, and W. Li, J. Mol. Liq. 311 (2020) 113312.
[61] J. Aljourani, K. Raeissi, and M. A. Golozar, Corr. Sci. 51 (2009) 1836.
[62] A. K. Singh, S. Mohapatra, and B. Pani, J. Ind. Eng. Chem. 33 (2016) 288.
[63] M. A. Bidi, M. Azadi, and M. Rassouli, Materials Today Commun. 24 (2020) 100996.
[64] M. Chellouli, D. Chebabe, A. Dermaj, H. Erramli, N. Bettach, N. Hajjaji, M. P. Casaletto, C. Cirrincione, A. Privitera, and A. Srhiri, Electrochim. Acta 204 (2016) 50.
[65] M. Chafiq, A. Chaouiki, M. R. Al-Hadeethi, I. H. Ali, S. K. Mohamed, K. Toumiat, and R. Salghi, Coatings 10 (2020) 700.
[66] M. Barral-Martinez, M. Fraga-Corral, P. Garcia-Perez, J. Simal-Gandara, and M. A. Prieto, Foods 10 (2021) 1793.

[67] F. O. Oshomogho, T. E. Akhihiero, O. Edokpayi, and J. E. Ossai, Glo. Jnl. Pure Appl. Sci. 26 (2020) 171.
[68] I. Oliveira, A. S. Meyer, S. Afonso, A. Sequeira, A. Vilela, P. Goufo, H. Trindade, and B. Gonçalves, Plants 9 (2020) 1627.
[69] I. Prgomet, B. Gonçalves, R. Domínguez-Perles, R. Santos, M. J. Saavedra, A. Aires, N. Pascual-Seva, and A. Barros, Ind. Crops. Prod. 132 (2019) 186.
[70] B. Nawade, M. Yahyaa, H. Reuveny, L. Shaltiel-Harpaz, O. Eisenbach, A. Faigenboim, I. Bar-Yaakov, D. Holland, and M. Ibdah, Plant Sci. J. 287 (2019) 110187.
[71] M. Boudalia, R. M. Fernández-Domene, M. Tabyaoui, A. Bellaouchou, A. Guenbour, and J. García-Antón, J. Mater. Res. Technol. 8 (2019) 5763.